

Video Article

An Analog Macroscopic Technique for Studying Molecular Hydrodynamic Processes in Dense Gases and Liquids

Jerry Dahlberg¹, Peter T. Tkacik¹, Brigid Mullany¹, Eric Fleischhauer¹, Hossein Shahinian¹, Farzad Azimi¹, Jayesh Navare¹, Spencer Owen¹, Tucker Bisel¹, Tony Martin¹, Jodie Sholar¹, Russell G. Keanini¹

¹Department of Mechanical Engineering, University of North Carolina at Charlotte

Correspondence to: Jerry Dahlberg at jdahlbe2@uncc.edu

URL: <https://www.jove.com/video/56632>

DOI: [doi:10.3791/56632](https://doi.org/10.3791/56632)

Keywords: Engineering, Issue 130, Macroscopic Molecular Liquid Hydrodynamics, Particle Image Velocimetry, Grain Physics, Dense Fluid Interactions, Statistical Mechanics, Continuum Mechanics, Vibrated Grain Pile

Date Published: 12/4/2017

Citation: Dahlberg, J., Tkacik, P.T., Mullany, B., Fleischhauer, E., Shahinian, H., Azimi, F., Navare, J., Owen, S., Bisel, T., Martin, T., Sholar, J., Keanini, R.G. An Analog Macroscopic Technique for Studying Molecular Hydrodynamic Processes in Dense Gases and Liquids. *J. Vis. Exp.* (130), e56632, doi:10.3791/56632 (2017).

Abstract

An analog, macroscopic method for studying molecular-scale hydrodynamic processes in dense gases and liquids is described. The technique applies a standard fluid dynamic diagnostic, particle image velocimetry (PIV), to measure: i) velocities of individual particles (grains), extant on short, grain-collision time-scales, ii) velocities of systems of particles, on both short collision-time- and long, continuum-flow-time-scales, iii) collective hydrodynamic modes known to exist in dense molecular fluids, and iv) short- and long-time-scale velocity autocorrelation functions, central to understanding particle-scale dynamics in strongly interacting, dense fluid systems. The basic system is composed of an imaging system, light source, vibrational sensors, vibrational system with a known media, and PIV and analysis software. Required experimental measurements and an outline of the theoretical tools needed when using the analog technique to study molecular-scale hydrodynamic processes are highlighted. The proposed technique provides a relatively straightforward alternative to photonic and neutron beam scattering methods traditionally used in molecular hydrodynamic studies.

Video Link

The video component of this article can be found at <https://www.jove.com/video/56632/>

Introduction

Molecular hydrodynamics studies the dynamics and statistical mechanics of individual molecules and collections of molecules within fluids. Among the many experimental techniques developed for studying molecular hydrodynamic systems^{1,2}, light scattering^{1,2,3}, molecular dynamic simulations^{4,5,6,7} and, to a lesser extent, inelastic neutron scattering⁸ have been most commonly used. Unfortunately, significant limitations attach to the latter two techniques. Molecular dynamics (MD) simulations, for example: i) are limited to small spatial and temporal ($\sim 10^{-9}$ to $\sim 10^{-6}$ s) domains containing relatively few molecules ($N \sim 10^3$ to $\sim 10^5$), ii) require use of approximate inter-particle potentials, iii) typically introduce periodic boundary conditions, invalid under non-equilibrium bulk flow conditions, and iv) cannot, at present, answer the fundamental question of how molecular-scale dynamics, involving either single molecules or collections of molecules, are affected by, and couple back to, bulk, non-equilibrium fluid flow. The main limitation associated with neutron scattering is tied to the difficulty of accessing the limited number of neutron beam sources available.

In order to provide context for the analog experimental technique presented in this article, we highlight light scattering techniques applied to simple dense-gas and liquid-state fluids. In a typical light scattering experiment, a polarized laser light beam is directed to a small interrogation volume containing a stationary fluid sample. Light scattered from molecules within the sample is then detected at some fixed angle relative to the incident beam. Depending on the molecular dynamic regime of interest, detection and analysis of the scattered light signal incorporates either light filtering or light mixing detection methods. As outlined by Berne and Pecora¹, filtering techniques, which probe fluid state molecular dynamics on time scales shorter than $\tau < \sim 10^{-6}$ s, introduce a post-scattering interferometer or diffraction grating, and allow scanning of the spectral density of the scattered light. Optical mixing techniques, used for slow-time-scale dynamics, $\tau > \sim 10^{-6}$ s, by contrast, incorporate a post-scattering autocorrelator or spectrum analyzer, in which the spectral content of the scattered signal is extracted from the measured scattered light intensity.

Generally, laser probes, at least those operating in the visible range of the spectrum, have wavelengths much longer than the characteristic spacing between liquid-state molecules. Under these circumstances, the probe beam excites five collective, slow-time-scale, long-wave-length hydrodynamic modes^{2,9,10} (slow relative to the characteristic collision frequency): two viscously damped, counter-propagating sound waves, two uncoupled, purely diffusive vorticity modes, and a single diffusive thermal (entropy) mode. The sound modes are excited in the (longitudinal) direction of the incident beam, while the vortical modes are excited in the transverse direction.

Considering purely experimental scattering techniques, two fundamental questions, lying at the heart of the equilibrium and non-equilibrium statistical mechanics of molecular, liquid-state systems, remain beyond light and neutron scattering measurements:

- 1) Rigorous arguments^{9,11} show that the random, collision- and sub-collision-time-scale dynamics of individual liquid-state molecules, subject to either classical Newtonian dynamics or quantum dynamics, can be recast in the form of generalized Langevin equations (GLE). GLE's, in turn, comprise a central theoretical tool in the study of the non-equilibrium statistical mechanics of molecules in dense gases and liquids. Unfortunately, since the dynamics of individual (non-macromolecular) molecules cannot be resolved by either scattering technique, there is presently no direct way, beyond MD simulations, to test the validity of GLE's.
- 2) A fundamental hypothesis lying at the heart of macroscopic continuum fluid dynamics, as well microscale molecular hydrodynamics, posits that on length- and time-scales large relative to molecular diameters and collision times, but small relative to continuum length- and time-scales, local thermodynamic equilibrium (LTE) prevails. In continuum flow and heat transfer models, like the Navier-Stokes (NS) equations, the LTE assumption is required⁹ in order to couple intrinsically non-equilibrium, continuum-scale flow and energy transport features — like viscous shear stresses and thermal conduction — to strictly equilibrium thermodynamic properties, like temperature and internal energy. Likewise, while microscale momentum and energy transport are intrinsically non-equilibrium processes, reflecting the appearance of coupled, microscale mass, momentum, and energy currents, models of these microscale processes assume that the currents represent small perturbations from LTE⁹. Again, to the best of our knowledge, there have been no direct experimental tests of the LTE assumption. In particular, it appears that no molecular hydrodynamic scattering experiments have been attempted within dense, moving, non-equilibrium fluid flows.

In this paper, we outline an analog experimental technique in which the macroscopic, single particle and collective particle dynamics of vibrated grain piles, measured using standard Particle Imaging Velocimetry (PIV), can be used to indirectly predict, interpret, and expose single- and multi-molecule hydrodynamics in dense gases and liquids. The physical and theoretical elements that enable the proposed technique are stated in a recent paper published by our group¹². Experimentally, the macroscopic system must exhibit: (i) a sustained tendency toward local, macroscale statistical mechanical equilibrium, and (ii) small, linear departures from equilibrium that mimic (weak) non-equilibrium fluctuations observed in molecular hydrodynamic systems. Theoretically: (i) classical microscale models describing the equilibrium and weakly-non-equilibrium statistical mechanics of dense, interacting N-particle systems must be recast in macroscale form, and (ii) the resulting macroscale models must reliably predict single- and multiple-particle dynamics, from short, particle-collision-time-scales to long, continuum-flow-time-scales.

Here, we present a detailed experimental protocol as well as representative results obtained by the new technique. In contrast to MD simulations and light and neutron scattering methods, the new technique allows, for the first time, detailed study of molecular hydrodynamic processes within flowing, strongly non-equilibrium, dense gases and liquids.

Protocol

1. Preparation of Vibratory System

1. **Set up the vibratory system as shown in Figure 1. This system consists of an annular polyurethane bowl (having an outer diameter of 600 mm), attached to a single-speed (1740 rpm), unbalanced motor, where the latter generates process vibrations. This is attached to a weighted base and separated by a group of eight springs (the bowl and weighted base are purchased assembled as one piece). Attach the bowl assembly to its stand and secure with two supplied rubber hooks. Place peristaltic pump on a table near the bowl and attach pump outlet hose to bowl lubrication inlet point.**
 1. Attach a triaxial accelerometer to the inner radius of the annular bowl to recorded bowl vibrations under low amplitude conditions and wire the accelerometer to a sensor signal conditioner. Place the signal conditioner on a table away from the vibratory system. The accelerometer/signal conditioner combination is controlled by data acquisition hardware/software installed on a standard computer.
2. **Prepare chosen media by washing in water and allowing to dry. Several types of media have been used during various experiments. For this paper, use a ceramic polishing media straight cut triangle (10 mm x 10 mm x 10 mm triangle as viewed from the front and 10 mm thick).**
 1. Determine the media packing density by first placing an empty plastic sack on a lab scale and taring the scale. Fill the plastic sack with the chosen media (not to exceed 18.927 L (5 gal) and record the weight of the media (g or kg). For this type of media and current experimental set up, the weight was 22.68 kg (50 lb).
 1. Place the bucket in a large sink, or outside of the building away from other equipment. Fill the bucket (For this set up, an 18.927 L (5 gal) bucket was used) with water to the full mark and slowly lower the plastic sack full of media into the bucket. Once the sack of media is completely submerged, slowly raise the bag from the water to avoid splashing and place the sack aside. Use a 1000 mL graduated cylinder to refill the bucket to its original full mark, recording the total amount of water added. This amount of water added will be V_p where V_p is the material packing volume of the media (For this set up, 13,750 mL of water was added back to the bucket). The amount of water added will be dependent on the type of media used.
 2. Calculate the media's packing density by the following equation:
$$\rho = \frac{m}{V_p}$$
 where ρ is the packing density of the media and m is the mass of the media (For this media, the density was calculated to be 1649 kg/m³).
2. Activate the vibratory system by plugging it into the electrical outlet (this model has two options, 1) plug into wall or 2) run with timer attached to stand). Activate data acquisition software on the computer by pressing the "Start" arrow on the user written program and gather data for 1 minute. Acceleration data will both be displayed for immediate review (in both the time domain and frequency domain) and automatically stored to a .csv file for potential post-processing. Unplug the unit from the electrical outlet to deactivate the vibratory system.
3. Add media to vibratory bowl.

4. Prepare compound, consisting of 3880 mL of water and 120 mL of finishing compound (FC) (3% volume) solution. Set peristaltic pump to 1.9 L/h (rotate speed dial to 27 to achieve this flow rate), but do not initiate flow. This will ensure that the solution is not recirculated, but is sufficient to keep the media wet. (This solution is a commonly used vibratory finishing solution). The solution acts as a lubricating agent and ensures the media does not stick together or wear down during the procedure.
5. Activate the vibratory system by plugging it into the electrical outlet. Gather accelerometer data as specified in Step 1.2.2. Unplug the unit from the electrical outlet to deactivate the vibratory system.

2. High Speed Imaging

NOTE: For grain velocity field measurements, obtained by imaging a portion of the surface of the flowing grain pile, the imaging area, A_I , corresponds to the field of view (FOV) determined in step 2.2.4 below. Measurement of time-varying, individual grain velocities (at the pile surface) can be obtained by choosing a small, fixed sub-area, δA_I , within A_I , where, as detailed below, δA_I is on the order of the projected area of an individual grain.

1. **Set up a high speed camera (The camera has 1504 x 1128 resolution up to 1,000 frames per second (fps)) to capture images by either placing it on a tripod or building a rigid frame with the lens perpendicular to the open surface of the vibratory system (when the bowl is vibrating) as seen in Figure 1. This rigid frame is separate from the vibrational system and ensures that the vibrations from the system do not affect imaging.**
 1. Attach appropriate lens for desired surface integration area and resolution. For the current set-up, use an 18 - 250 mm zoom lens with and a lens ratio of 1:3.6 - 6.3. Attach power supply and GPS antenna to camera. Attach camera to computer using a CAT5 cable. Place the camera so that the end of the lens is approximately 550 mm above the surface of the media.
NOTE: Placing the camera too close to the media will cause increased edge effects and placing the camera too far away will cause the images to be too dark to process. At the specified distance, errors due to edge effects and overall curvature of the test area is <2%.
 2. Remove lens cap and start camera software. When it has started, click on "Cameras" button, and then click OK. When camera list populates, select the camera from the list and click open.
 3. In the camera software on the computer, under "Live" tab, click "Live" button (blue arrow) to view the camera's FOV. Turn on the light source to illuminate the region to be imaged. This can be any bright light as long as it illuminates the test area evenly. **Figure 1** shows the camera and light configuration with respect to the vibratory system.
 4. To determine the f-stop, look at the computer screen with the live stream from the camera and adjust the f-stop to its minimum setting (maximum brightness). If the f-stop is set to low, the result is a shallow depth of field. If the f-stop is set to high, the screen is too dark. For this experiment, the f-stop was set to 3.6.
 5. Adjust focal length on lens to provide the desired FOV (210 mm x 160 mm for this case). For this experiment, set the focal length at 180 mm with the camera set 550 mm above the media surface. **Figure 2a** shows the FOV through the camera.
 6. Digitally zoom in to 500X magnification using the camera software. Adjust the focus ring on the lens for best optical focus. Return digital zoom to 100% (Normal view).
 7. Under Acquisition Settings on computer, click "Rate [Hz]" and set to 500 frames per second .
NOTE: In order to resolve grain-collision-time-scale dynamics, f_{frame} must be at least an order of magnitude larger than the imposed vibration frequency, f_o . (Here, $f_o = 29.3$ Hz)
 8. Prior to taking images, place a ruled scale in the field of view; this provides a length scale for subsequent image data processing. Under Acquisition Settings on camera software, select "Record" tab under "Live". Set "Record Mode" to "Circular" and Set Frames to 1. Click red circle under "Live" tab to record a single image as seen in **Figure 2b**.
 9. Save the acquired image as a TIFF file to a convenient file directory location (e.g. external hard drive) by clicking "File", and then click "Save Acquisitions". A dialog box will appear with multiple options. Next to file type in the dialog box, select .tiff from the drop-down menu.
 1. Select "Download Options" tab at the bottom of the dialog box and click "Browse". At the top of the dialog box, add the folder name for the test. In the "Browse" dialog box, search for and choose desired location (e.g. external hard drive) and appropriate folder. Once folder has been selected, click "OK" then "Save". The download manager box will appear. The file will begin to transfer and be saved in the file location specified in subfolder 001. Once the image has transferred, a "Done" status box will appear on the screen.
 2. Delete image from camera by clicking the red delete button.
NOTE: The protocol can be paused here.

3. Gathering Data

NOTE: If the protocol was paused, the camera will need to be restarted. Follow step 3.1. If protocol was not paused, skip to step 3.1.2.

1. **Start camera software and turn on illumination as specified in Step 2.**
 1. With camera software activated, check light conditions and run live as detailed in step 2.2.2. to ensure proper focus.
 2. Choose a total experimental run time, t_{exp} .
NOTE: Two competing requirements must be met: i) t_{exp} must be long enough that statistically stationary grain flow conditions set in, and ii) t_{exp} should not be so long as to produce large amounts of superfluous data. The time scale on which stationary conditions appear must be determined by trial and error. Various methods, of varying rigor, can be used. For example, i) ensure that the time average grain velocity at a fixed point, or at multiple fixed points, reaches a nominally fixed magnitude or magnitudes, or ii) ensure

that, in addition to stationary means, corresponding variances also assume nominally fixed magnitudes. For this experiment, data was collected for 10.12 s, corresponding to acquisition of 5060 frames. Steady conditions in the grain flow set in after approximately 1 s.

2. Activate Vibratory Bowl.

1. Spread 150 mL of finishing/lubricating compound (Step 1.2.4) evenly around the bowl to provide initial wetting of the media; and then place jug with remaining compound on the floor with a hose attached to the peristaltic pump. Activate the peristaltic pump (as set in Step 1.2.4) by flipping the switch from "off" to "clockwise".
2. Turn on vibratory bowl by plugging it into an electrical outlet and wait a minimum of one minute to ensure even wetting and steady fluid motion throughout the media (steady fluid motion occurs when the flow of fluid entering the bowl from the peristaltic pump is approximately equal to the flow of fluid draining from the bowl drain).

3. Capturing Video and Gathering Data.

1. Once fluid reaches steady motion (Step 3.2.2), trigger the camera by clicking the red record icon on the computer screen and then click the red trigger checkmark to record images for the chosen time duration, t_{exp} . The camera will record images for the specified t_{exp} and save those images to its internal memory. **Figure 2a** is an example of a single image out of a set of 5060 images taken.
2. Once data is collected, shut down vibratory system by unplugging it from the electrical outlet and deactivate the peristaltic pump by flipping the switch from "clockwise" to "off".

NOTE: The protocol can be paused here.

4. Process Video Data with PIV

1. Prepare the high speed camera images for PIV processing.

1. Save the acquired images as TIFF files following the procedures outlined in Step 2.1.9. (In the current system, 5060 image frames collected over 10.12 s takes over an hour to transfer). Once images are transferred, a "Done" status box will appear on the screen. The files will be saved in the same directory as the calibration file in a subfolder identified as 002. Delete images from camera.
2. Convert the color images into grayscale images to enable processing by the PIV software. Upload the images into the data analysis software by using an "imread()" function. Convert a copy of the images using the "rgb2gray()" function and save/write these new images into a new folder using the "imwrite()" function.

NOTE: This process/data analysis function is available for multiple types of data analysis software and is written as a complete program by the researcher. **Figure 2c** is an example of a zoomed in image after it has been converted to grayscale and been processed by PIV.

2. Use PIV software to calculate velocity fields.

1. Use the import wizard to import the set of grayscale images as single frame images into the PIV software environment. Begin the import by clicking on "File", and then select "Import" and "Import Images". The image import wizard dialog box will appear. Choose "Single Frame" import option from the menu and click "Add Images" button. Select calibration image and click "Open", which adds the image to the "Images to Import" dialog list box. When importing images, add the calibration image (Step 2.1.9) first so that it is the top image in the import list. Click "Add Images" button again and highlight all data images and click "Open" to add them to the "Images to Import" dialog box. Click "Next" once all the desired images are selected. Input the camera settings used, include frame rate and pixel pitch in the dialog boxes. Click "Next" and "Finish" to complete the import process.
2. Separate the calibration image from the image set and input length scale parameters into the PIV software.
 1. If the contents list is not already displayed, right click the imported image set and select "Show Contents List" on the left side of the screen in the data base tree. Assuming the calibration image was the first imported image, right click the second image in the list and select "Split Ensemble from Here". Drag and drop the newly created image set (containing only the calibration image) to the location on the left of the screen labeled "New Calibration".
 2. Right click the newly placed calibration image set and select "Measure Scale Factor". When the calibration image appears on-screen, position the "A" and "B" markers on the in-image ruler (or other object of known size if ruler was not used) and input the distance between the markers in the "Absolute Distance" text box. Click "OK" on the "Measure Scale Factor" dialog box, which will save the calibration setting and close the dialog box and the calibration image.
3. Create a set of image pairs by selecting the imported image set and click "Analyze". Next select "Make Double Frame" from the list of available analysis methods. Choose "(1-2, 2-3, 3-4,...(N-1) double images)" style option.
 1. Open any image in the image set (except calibration image) and right click on image and select "Particle Density". A dialog box showing recognized particles will appear on the screen. It will show a zoomed in view of a probe area. Click settings tab on this dialog box and alter "Probe Size Area" until a minimum of 3 particles are consistently seen in the probe area. This probe area size will be the interrogation area size entered in step 4.2.5.
4. Use the "Analyze" command on the selected image set to choose PIV processing algorithm and associated parameters. Select the "Adaptive Correlation" method and define the area of pixels which will be used to define a vector in space in step 4.2.5. (This process divides images into a grid of $n \times n$ pixel "Interrogation Areas")
5. Set the interrogation area size by locating the "Interrogation Areas" tab and selecting any of the available interrogation area sizes between the minimum of 8 pixels and the maximum of 256 pixels (For this method, 32 pixels by 32 pixels was used). Enter the value determined in step 4.2.3.1.
 1. To increase the density of vectors created, add Interrogation area "Overlap" percentage by choosing 0%, 25%, 50% or 75% overlap from the drop-down menu.
6. Perform analysis leading to measured grain velocity field by selecting "OK" in the "Adaptive Correlation" dialog box. The system will begin analysis. As the system processes the data, the first vector map will appear on the screen. Inspect the first several velocity fields to determine if they appear satisfactory by estimated velocity and direction as seen in **Figure 2c**. If the velocity field does not appear

realistic, cancel the analysis session, repeat Step 4.2.4, and change analysis settings. (When the analysis is completed, a vectoring field, spanning the FOV, will be created for each image pair in the set (Step 4.2.3)). **Figure 2c** shows an example satisfactory vector field during the analysis process that has been overlaid on a greyscale image.

NOTE: For each $n \times n$ pixel interrogation area, the PIV software compares the pattern of sub-grain-scale bright spots within the interrogation area against corresponding patterns captured in the next image. From this comparison, the PIV software determines an area-averaged displacement vector, $\Delta \mathbf{r}_i$, and finally, by dividing $\Delta \mathbf{r}_i$ by the time increment between frames, $\Delta t = f_{frame}^{-1}$, the area-average velocity, $\mathbf{v}_i = \Delta \mathbf{r}_i \Delta t^{-1}$, where i refers to interrogation area i . In the current experiments, each interrogation area consisted of $n \times n = 32 \times 32$ pixels; the total number of interrogation areas subdividing each 210 mm x 160 mm FOV was thus 47 x 35, corresponding to 1504 x 1128 pixels.

5. Process Vibrational Data

NOTE: Step 5 may be done simultaneously with Step 4 if different computer systems or analysis software is used.

1. **Open data analysis software and by using the "load()" function to bring in the accelerometer data that was acquired when the vibratory bowl was empty (Step 1.2.2). Do a fast fourier transform of the data using the "fft()" function. Create a figure of the data using the "plot" function. Repeat with the data that was acquired when the vibratory bowl had media present (Step 1.2.5).**

NOTE: This process/data analysis function is available for multiple types of data analysis software and is written as a complete program by the researcher.

1. In order to study molecular hydrodynamic processes, a number of data processing operations are generally required. See the Representative Results and Discussion sections below for outlines of the main processing procedures; see Keanini, *et al.* (2017)¹² for details on how measured PIV data can be used to extract dynamical information on molecular hydrodynamic systems.

Representative Results

In presenting representative results, we refer to *continuum-time-scale* processes as those observed and predicted over time-scales, τ_L , that are long relative to the characteristic grain collision time scale, $\tau_c = f_o^{-1}, \tau_L \gg \tau_c$, and *particle-time-scale* processes as those observed and predicted over time-scales, τ_S , that are on the order of, or smaller than $\tau_c, \tau_S \lesssim \tau_c$ where f_o is the vibration frequency of the grain media container.

The proposed technique provides simultaneous, integrated, superposed experimental information on single-particle and multiple-particle, random and time-averaged dynamics extant over time scales ranging from the inverse PIV camera sample rate, $\tau_{min} = f_s^{-1}$, to the length of any given experimental run, $\tau_{max} = t_{exp}$. For the results presented here, $f_s = 500$ camera frames per second and $t_{exp} = 10.12$ s.

The results are organized as follows. First, we show, using a representative video clip, that all measurements are obtained under strongly non-equilibrium conditions in which the vibrated grain media move in collective, fluid-like flow; see **Supplemental Movies 1a-c**. The existence of local thermodynamic equilibrium, LTE, observed at an arbitrary, spatially limited camera interrogation area on the surface of the granular flow, is then demonstrated; see **Figure 3**. Evidence of weak non-equilibrium departures from LTE — taking place on individual particle scales, and produced by the cyclic injection of vibrational energy into the grain media — is then presented; see **Figure 4**. Finally, as a means of demonstrating that long-time-scale, non-equilibrium granular flows can be reasonably predicted using coarse-grained versions of exact, discrete, particle-scale mass and momentum conservation laws, here, the Navier-Stokes (NS) equations, we present a comparison of observed time-averaged grain flow fields against those predicted by the NS equations; see **Figure 6**.

In our experiments, we investigate the vibration-driven dynamics of eight different grain media, each media type characterized by a given shape, or mixture of shapes, mass density, and characteristic, fixed set of dimensions. In all experiments, the media bowl is filled with a fixed total mass of grain media, and the vibration frequency and amplitude of the bowl are fixed at 29.3 Hz and 2 mm, respectively. As depicted in supplemental movie 1a, observed grain flow patterns, are for all eight media, qualitatively similar: a slow, steady, three-dimensional helical flow, reflecting a dominant, radially-inward component, in which media flows from the outer bowl boundary radially inward toward the bowl's inner boundary, combined with a weak azimuthal component. Thus, in contrast to light- and neutron-scattering measurements, measurements of single-particle- and multi-particle-scale statistical mechanics must here be carried out in the presence of non-equilibrium flow.

Vibrated grain systems allow what we believe to be the first experimental demonstration of local thermodynamic equilibrium within non-equilibrium fluid flows. As shown in **Figure 3**, normalized histograms of measured horizontal peculiar grain speeds, obtained at a fixed 4 mm x 4 mm interrogation area on the grain pile surface, are well-fit by Maxwell-Boltzmann (MB) distribution functions. MB distributions, in turn, provide strong evidence of several fundamental dynamical properties: i) they are consistent with the existence of collision-time-scale (dissipationless) Hamiltonian dynamics, ii) they are likewise consistent with existence of velocity-independent interparticle potential energies, as well as a potential-independent kinetic energies, and iii) they provide strong evidence of local, macroscopic, mechanical equilibrium. Importantly, all of these features can be interpreted as macroscale embodiments of dynamical properties traditionally assumed in equilibrium liquid-state molecular hydrodynamic systems.

In order to expose the statistical mechanics of individual grains, the local *peculiar* grain velocity must be extracted from the measured local grain velocity: i) First, periodic spectral components within the local measured velocity, reflecting solid-like elastic vibration of the grain pile, must be filtered from the (PIV-) measured, time-varying velocity observed at the interrogation point. ii) Next, the local *filtered* velocity record, representing the purely fluid-like flow component of the grains' dynamics, is used to determine the local, time average velocity (over the entire experimental period, $0 < t \leq t_{max}$). iii) Finally, the local average (filtered) velocity is subtracted from the time-varying local filtered velocity. The resulting time-varying velocity record thus represents the *local peculiar fluid velocity*, as observed at the interrogation point.

Beyond a tendency to revert, at all locations, toward LTE, macroscopic dynamical systems – if they are to serve as true analogs of liquid-state molecular hydrodynamic systems - must possess a second set of crucial property: weak random fluctuations from local equilibrium, taking place on collision and sub-collision-time-scales, that are consistent with generalized Langevin dynamics. Here, as shown in **Figure 4**, the normalized single-grain (peculiar) velocity autocorrelation function, $\psi(t) = \langle v(t) \cdot v(0) \rangle \langle v(0) \cdot v(0) \rangle^{-1}$, exhibits the same qualitative structure long-predicted in MD simulations of dense gases and liquids^{2,13}: i) a rapid, non-exponential, sub-collision-time-scale decay to slightly negative values, followed by ii) an extended, slow, approach back toward zero. Physically, and again consistent with MD-predicted single-molecule dynamics in dense fluids^{2,4} the long negative tail in shown in **Figure 4** appears to reflect the collective influence of neighboring grains on the motion of individual grains¹². In theoretical terms, the short-time-scale temporal structure of $\psi(t)$ is fully consistent with, and explainable in terms of, generalized Langevin dynamics².

Another dynamical ingredient necessary to establishing a predictive macroscopic analog to liquid-state molecular hydrodynamic systems centers on collective hydrodynamics. First, on long time-scales – long relative to f_o^{-1} - and on large length-scales – large relative to the characteristic grain dimension, d_g - macroscopic system hydrodynamics must exhibit the same modal response structure predicted and observed in liquid-state molecular systems^{2,9,10}. As noted above, the response of dense fluid systems to both spontaneous fluctuations and externally-imposed disturbances - for example, particle beams in scattering experiments and small-amplitude vibrations in our experiments – consists of two viscously-damped counter-propagating sound modes, two, uncoupled, diffusive vortical modes, and a diffusive thermal (entropy) mode. Second, the long-time-scale, large-length-scale collective dynamics of macroscopic N-particle systems must – as molecular systems do – follow the NS equations (including, again, mass and energy conservation).

At present, with respect to macroscopic modal response, we have only indirect experimental evidence of damped *fluid-state* acoustic modes: as shown in **Figure 5**, *solid-state* acoustic standing waves, driven at the imposed vibration frequency, f_o , as well as at harmonics of f_o , are observed in our vibrated grain piles. Unfortunately, due to limitations in the present experimental system, we do not observe acoustic modes in spectra of the local peculiar *fluid* velocity. In order to excite such modes, new experiments will be carried out in which the media bowl will be subject to cyclic impact. Based on the unambiguous existence of solid-state acoustic modes, we anticipate that this approach will expose fluid-state acoustic modes.

By contrast, we have strong evidence that the collective, macroscopic, long-time and large-scale dynamics of vibrated grain piles do obey the NS equations. As shown in **Figure 6**, PIV-measured steady state velocity distributions measured on the surface of a vibrated pile are well predicted by the NS equations¹⁴. Here, as detailed in Mullany *et al.*¹⁴, the equations are solved numerically within a rectangular, two-dimensional domain corresponding to the surface FOV used in PIV velocity field measurements¹⁴. The simulations use experimentally measured effective grain viscosities and impose spatially-varying velocity boundary conditions, determined by PIV measurements, on three of four domain boundaries. Although the simulation assumes strictly two dimensional flow, where the actual flow is three-dimensional, and neglects the presence of the media bowl's central hub (the latter giving the bowl a donut/toroidal shape), average errors between predicted and actual velocity magnitudes are only on the order of 15%.

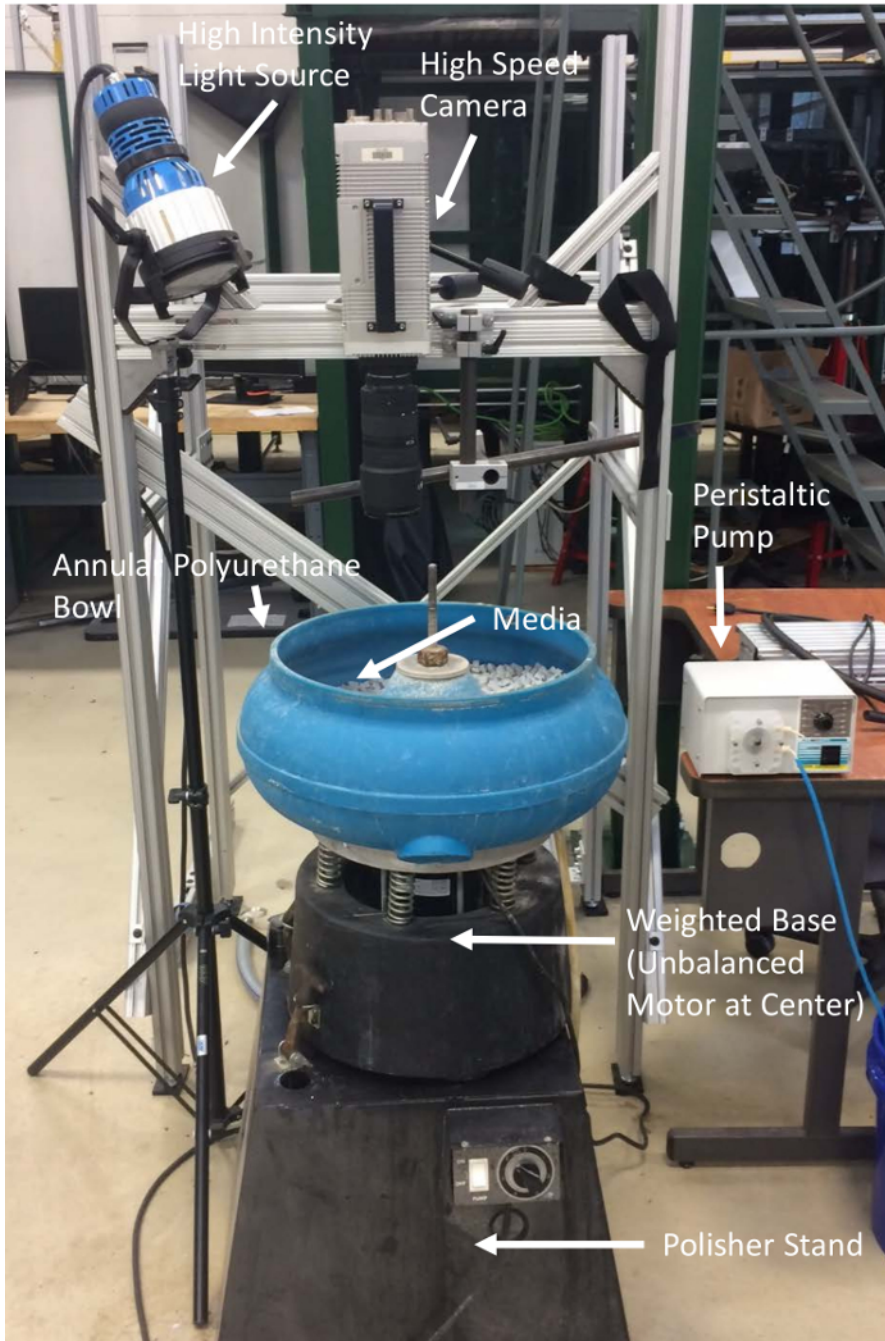


Figure 1: Vibratory System Experimental Set-Up with Camera and Lighting. This system consists of an annular polyurethane bowl having an outer diameter of 600 mm, with a single-speed (1740 rpm), unbalanced motor. The camera and lighting system are suspended above the vibratory bowl and attached to support structures or tripods not in contact with the vibratory system. This ensures that the motion of the bowl does not cause movement in the camera or the light. The peristaltic pump provides steady fluid flow to lubricate the media. [Please click here to view a larger version of this figure.](#)

Supplemental Movie 1: Typical Grain Flow Video. (a) A typical clip of the grain flow as captured by the high speed camera. (b) Slow motion video of media undergoing tangential flow around a stationary workpiece (c) Slow motion video of media undergoing normal flow into a stationary workpiece. The PIV-measured velocity fields in (c) are compared against theoretically computed velocity fields in **Figure 6**. [Please click here to download these files.](#)

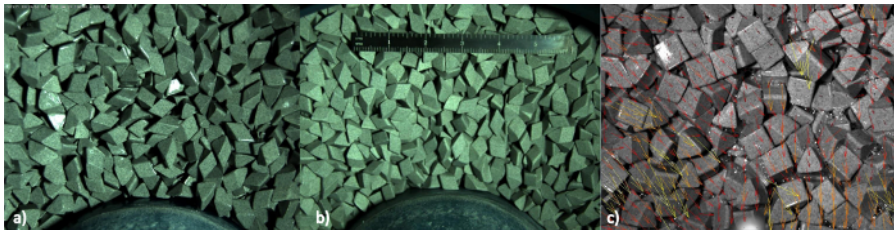


Figure 2: Example Processing and Post Processing Images. (a) A typical FOV single image taken by the high speed camera. (b) A typical calibration image with a scaled ruler. (c) Zoomed in view of velocity vector map overlaid on the first frame of the double frame images used to calculate the vectors. The vectors represent the particle movement between first and second frames of the double frame. The velocity ranges from ~0 m/s (dark red) to 0.17 m/s (yellow) in this figure. [Please click here to view a larger version of this figure.](#)

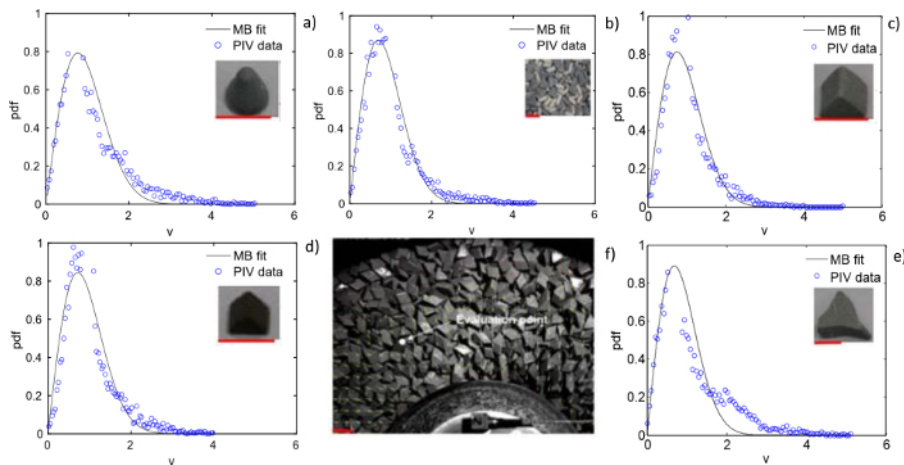


Figure 3: Experimental evidence of local statistical mechanical equilibrium. Distributions of horizontal peculiar (random) grain speeds, measured at the point shown in (f), are fit by two dimensional Maxwell-Boltzmann (MB) speed distributions. (a-e) depicts Speeds (v), and probability density functions (pdf) are in units of cm s^{-1} and s cm^{-1} , respectively, and the red scales represent 1 cm by grain type. The grains shown are: (a) RS19K; (b) mixed media; (c) RS1010; (d) RCP0909; and (e) RS3515. This figure has been modified from Keanini *et al.* in Science Reports (2017)¹². [Please click here to view a larger version of this figure.](#)

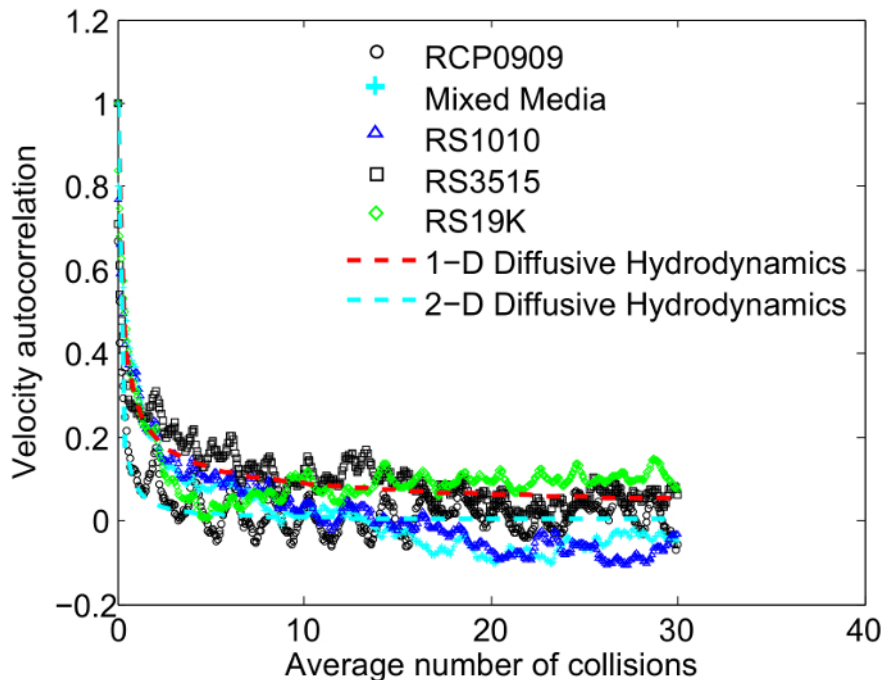


Figure 4: Single grain, short-time-scale dynamics. The velocity autocorrelation function, $\psi = \psi(N_c)$, for single grains, plotted as a function of the characteristic number of grain collisions, $N_c = t f_o^{-1}$, where t is the time lag and f_o is the vibration frequency. Collision-time-scale, single grain dynamics exhibit trends qualitatively mimicking those predicted in molecular liquids and dense gases, including: (i) trapped particle dynamics, here determined by the continuum response of the grain fluid to vibrational forcing¹², (ii) rapid, non-exponential decay in $\psi(t)$, consistent with generalized Langevin dynamics¹², and (iii) manifestation of dense gas, liquid, and mixed liquid-solid thermodynamic phases¹². This figure has been modified from Keanini *et al.* in Science Reports (2017)¹². [Please click here to view a larger version of this figure.](#)

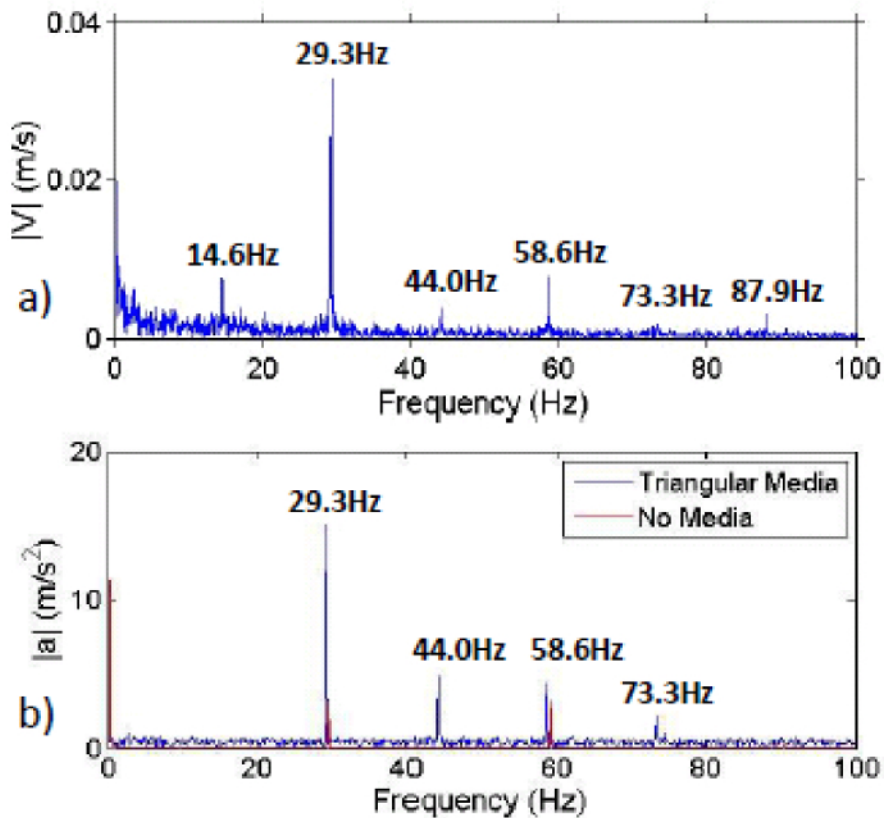


Figure 5: Vibrational response to vibration. Amplitude spectra¹⁵, determined from local PIV grain velocity measurements and from simultaneous container acceleration measurements, are shown in (a and b), respectively. The PIV measurement location is shown in **Figure 3f**; grain container accelerations are obtained from the exterior of the container. Resonant acoustic waves within the grain pile-container system, manifested by peaks in the spectrum (a), nominally coincide with resonant acoustic modes excited within the empty container, shown in (b). The fluid dynamics of both individual grains and of the entire grain pile are exposed by filtering the solid-like acoustic response. This figure has been modified from Keanini *et al.* in Science Reports (2017)¹². [Please click here to view a larger version of this figure.](#)

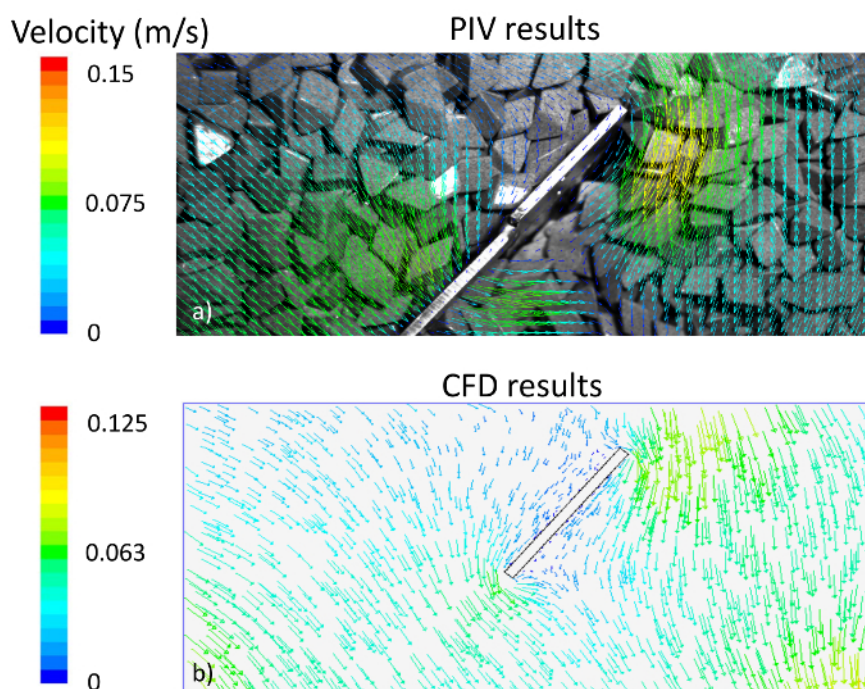


Figure 6: Comparison between PIV measured and PIV predicted velocity fields. (a) PIV- measured velocity field for normal flow around a stationary workpiece (FOV has been limited to 91 mm x 198 mm to match the CFD specified area) overlaid on image of vibrating media used to create the vector map ; (b) CFD-predicted velocity field for normal flow around stationary workpiece. This figure 6b has been modified from the MSME thesis of J. Navare¹⁶. [Please click here to view a larger version of this figure.](#)

Discussion

In order to use vibrated grain piles as macroscopic analogs for investigating molecular hydrodynamic processes, an experimentalist must, on one hand, learn and use four basic measurements, and on the other, master a few basic elements of equilibrium and non-equilibrium statistical mechanics. Focusing first on experimental measurements, these include: i) measurement of individual grain dynamics through measurement of the single-particle velocity autocorrelation function, ii) measurement of time-average/long-time-scale surface grain velocity fields, iii) measurement of grain media effective viscosities, and iv) measurement of the vibration spectra of the media bowl, both empty and filled with media.

Measurement of single particle velocity autocorrelation function

The random dynamics of individual particles, either molecules in microscale systems or vibrated grains in the present method, are studied via measurement of the single particle velocity autocorrelation function, $\psi(t)$ ². For small, e.g., diatomic and triatomic molecules, $\psi(t)$ in molecular liquids can only be determined through MD simulation^{2,6,7}. By contrast, $\psi(t)$ for individual grains in liquid-like vibrated grain piles can be experimentally determined. Specifically, in order to reliably measure $\psi(t)$, the number of images, N_I , obtained for any given grain passing through the chosen (camera) interrogation area, A_I , should be on the order of, or should exceed the characteristic number of grain collisions, N_C , required for $\psi(t)$ to decay from an initial magnitude of 1, $\psi(0) = 1$, to some small, near-zero magnitude. For grains that exist in an effective liquid state¹², $\psi(t)$ decays rapidly to slightly negative magnitudes – see, e.g., **Figure 4** – and then slowly reapproaches zero. Under these circumstances, N_C can be estimated as the characteristic number of grain collisions that occur up to the instant, t_0 , when $\psi(t = t_0) = 0$; thus, $N_C \approx t_0 f_0^{-1}$, where f_0 is the imposed grain bowl vibration frequency. Finally, N_I can be estimated as $N_I \approx L_I V_I^{-1} f_{frame}$, where L_I represents either the side-length of the (square) interrogation area, $A_I = L_I^2$, or a characteristic dimension associated with A_I , V_I is the (PIV-) measured time-average velocity magnitude at the centroid of A_I , and f_{frame} is the camera frame rate. Note, in our experiments, $L_I = 4 \text{ mm}$, $A_I = 16 \text{ mm}^2$, $V_I \cong 20 \text{ mm s}^{-1}$, $f_0 = 29.3 \text{ Hz}$, $N_C \approx 2$, $f_{frame} = 500 \text{ fps}$, so that $N_I \approx 100$ and, thus, $N_I \gg N_C$.

Measurements required to expose granular liquid state hydrodynamics

Elastic wave modes, specifically phonon modes, excited by both external means and by random thermal fluctuations, are known to exist in liquids^{17,18}. As shown in **Figure 5**, vibrated grain piles likewise exhibit solid-like elastic response to vibrational forcing. In order to isolate the fluid-like properties of a vibrated grain pile, two measurements must be performed: i) elastic wave modes within the pile must be identified by measuring the acceleration spectrum of the media container, under both (media-) loaded and unloaded conditions, and ii) the time-average grain

velocity must be measured, either at the centroid of a small interrogation area if investigating liquid-state dynamics of individual grains, or over a (much) larger interrogation area if studying the collective, continuum dynamics of the grain fluid flow field.

Once these measurements are obtained, and then as detailed in Keanini *et al.*¹², the purely elastic/solid-like spectral components of the PIV-measured total velocity – either for single grains or for collections of grains – is filtered from the measured spectra of the total, location- and time-dependent velocity. Importantly, the result is assumed to represent the purely fluid-like dynamics of the vibrated grains. Given the location- and time-dependent filtered grain fluid velocity – at a point or over an extended area – then, depending on the task, a number of straightforward data processing procedures can be performed. For example, if one is interested in comparing observed continuum grain flow fields against those predicted by a given hydrodynamic model, e.g., the NS equations, and then the location-dependent time-average velocity field can be determined by simply computing the time average of each location-dependent, time varying, filtered velocity. See, for example, Figure 6, above. If the dynamics of the location- and time-dependent peculiar, *i.e.*, random velocity field are of interest, the location-dependent time-average (filtered) velocity is subtracted from the location- and time-dependent (filtered) total velocity. This processing step is required, for example, in order to determine single particle velocity autocorrelation functions, $\Psi(t)$. See for example, Figure 4.

Finally, the effective dynamic or kinematic viscosity, μ or ν , where $\nu = \mu\rho^{-1}$, and ρ is the effective grain fluid density¹⁴ represents the central non-equilibrium hydrodynamic transport property associated with vibrated grain flows. For example, experimentally- or theoretically-determined values of μ or ν are required in computational hydrodynamic simulations of grain flows. From a fundamental standpoint, experimental values of μ or ν are needed in order to validate statistical mechanical predictions of these properties¹². Importantly, our group will soon report a straightforward viscometric technique for measuring effective dynamic and kinematic viscosities for a large family of vibrated grains, as observed in our experimental system.

Theoretical elements

In this section, we highlight a minimal set of theoretical ideas and methods an experimentalist should become acquainted with when attempting to use vibrated grain piles as an analog for studying and predicting the molecular hydrodynamics of molecular liquid systems. The following applies to classical, as opposed to quantum liquid systems; suggested references are, in most cases, representative of large numbers of papers, monographs, and books. These ideas and methods are most commonly separated into two categories, equilibrium and non-equilibrium statistical mechanics of N-particle systems.

In equilibrium statistical mechanics, the experimentalist needs to first model the system Hamiltonian¹⁹. The Hamiltonian describes the collision- and sub-collision-time-scale dynamics of the N-particle system, and typically consists of a term modeling the system's total translational kinetic energy, a term modeling the system's total potential energy, and in cases where particles undergo significant rotational motion, a term capturing the total rotational kinetic energy. In order to connect the Hamiltonian dynamics of the N-particle system to associated equilibrium thermodynamic functions, such as the system internal energy, or the effective system temperature or pressure, one typically next chooses an appropriate statistical ensemble. For N-particle systems, such as those studied in this paper, which are excited by a nominally fixed source of energy - here, multimodal vibration produced by a single frequency motor - the fixed energy microcanonical ensemble^{19,20,21} is appropriate. However, since thermodynamic calculations, such as calculation of the system entropy, are typically difficult in this ensemble, the canonical ensemble¹⁹ is generally a better choice and, moreover, produces the same equilibrium thermodynamic functions obtained via the microcanonical ensemble.

Given the system Hamiltonian and a chosen statistical ensemble, one then constructs the system partition function $Q = Q(N, V, T)$ ^{19,23}, where V and T are the system's equilibrium volume and temperature. Physically^{19,23}, Q contains all possible energy states, that, in principle, are accessible to the system. Practically, given Q , and given the so-called Bridge Relations^{19,23} connecting discrete N-particle system dynamics to an equilibrium thermodynamic function^{19,23}, and then all equilibrium thermodynamic properties associated with the N-particle system can be calculated. We highlight an additional point: In interacting systems, such as high-restitution grain piles driven by low-amplitude vibration¹², the pair correlation function^{9,19} typically appears (in the partition function, Q) and must be determined in order to determine equilibrium thermodynamic properties.

Non-equilibrium statistical mechanics studies spontaneous, *i.e.*, thermal, and non-spontaneous, externally-imposed departures from local thermodynamic equilibrium, where the latter arise due to spatial gradients in mass, momentum, and/or energy. In order to interpret and predict non-equilibrium dynamics of vibrated grain systems, and assuming weak departures from local equilibrium - the picture assumed, for example, in continuum fluid flows governed by the NS equations - four theoretical tools should be learned and mastered.

First, considering the non-equilibrium dynamics of individual grains, the GLE, and the simpler, memory-free Langevin equation (LE)^{2,9,11} provide a rigorous basis for studying this feature. In particular, short, collision-time-scale, single-grain dynamics, in dense liquid-like states¹², are best modeled using the GLE, while on longer time scales - from, say 10 collision times and longer - the LE, describing Brownian particle dynamics, is appropriate¹².

Second, in order to predict effective grain viscosities, as well as effective grain self-diffusion coefficients² - the first, an essential transport property required for accurately modeling the continuum flow of vibrated grain fluids, the Green-Kubo relations^{2,9,23} are available. In order to apply the Green-Kubo relations, an experimentalist should learn how these are derived; relatively straightforward derivations can be found, for example, in Boon & Yip².

The third tool required for studying the non-equilibrium statistical mechanics of vibrated grain systems corresponds to a rigorous coarse graining procedure^{9,12} that recasts the exact, discrete-particle versions of the mass, momentum and energy conservation laws into continuum, *i.e.*, NS, form. The procedure thus constitutes the essential bridge for rigorously deriving the continuum equations governing the fluid-like, collective dynamics of vibrated grain systems, as well as the conceptual basis for understanding the intimate connection between local equilibrium thermodynamic properties, like pressure, temperature, sound speed, and specific heat, to the non-equilibrium, continuum transport of mass, momentum, and energy.

Fourth, in order to expose and interpret large-length-scale, hydrodynamic modes^{2,9} that pervade both molecular liquid and vibrated grain systems¹², an experimentalist should become acquainted with the analysis of these modes. Briefly, the continuum response of molecular

liquids to scattering beams^{1,2,9}, and likewise, the continuum response of grain piles to vibration¹², reveals the existence of five, coupled, linear (*i.e.*, weak), collective modes. The modes arise from the five, coupled, continuum mass, momentum and energy conservation equations, and physically, reveal the modal processes that communicate spatial differences in conserved properties. These spatial differences, in turn, drive continuum transport of these properties.

Modifications and trouble shooting

For the PIV measurements, the bowl diameter could be modified (increased) to the point where the field of view of the camera is perpendicular over a nearly flat section of the test area which would remove more of the edge effects. Additional methods could be added to measure other variables such as force or pressure.

The mechanical pieces of the experimental set up are robust and require very little trouble shooting. If the media appears to be sticking together, the FC solution rate may be increased to ensure relatively smooth motion.

A majority of the trouble shooting would be in the PIV or data analysis systems. The first common problem occurs when the images are not imported in correct sequence. An image set may be sorted incorrectly in a computer file system if it is numbered using both negative and positive numbers, as is the case if the camera is set to trigger after obtaining an initial buffer of images. A file system may place the negatively numbered images directly beside their corresponding positively numbered image, which will cause the image set to import into the PIV software environment in a wrong order, which in turn leads to improper creation of double frames. Re-label the images using only positive numbers to ensure they are sorted in proper sequence.

If the PIV system gives errors when importing the images, it is most likely due to the images being in the wrong format. Ensure images are grayscale using data processing software and saved in TIFF format before importing into the PIV software environment.

Calibration errors can also be common, but not always recognized until the processing is complete. The PIV software environment separates imported image sets into "Runs," each of which has its own unique calibration. Therefore, each new run must include a calibration image (Step 2.2.7). Calibration images may only be re-used between runs if there is absolutely no change to the experimental setup or field of view. A new set of images may be imported into an existing run if said run is selected prior to starting the import process (Step 4.2.1). This will allow the new image set to use the run's existing calibration image, but should only be done if all image sets in the run are captured using the same camera.

Limitations

The main limitations of the PIV measurement technique, in its present configuration, is that it cannot measure the vertical grain velocity component, perpendicular to the grain bed's nominally horizontal free surface. Our observations, however, indicate that the long-time-scale, continuum grain flow remains essentially horizontal at the free surface, while the vertical, short-time-scale, random (peculiar) velocity component is likely of the same order of magnitude as the (two) measured horizontal peculiar components. Thus, this limitation has little impact on analysis of the grain bed surface's continuum flow, while it is reasonable to assume that the short-time-scale vertical random motion shares the same statistical properties as those measured for the horizontal components¹².

Significance with respect to existing methods

To our knowledge, this is the first study to demonstrate that vibrated grain piles can be used as a predictive analog for studying liquid-state molecular hydrodynamic processes. There are two approaches for studying molecular-scale dynamics in dense liquids and gases, one of which measures light, neutrons, or high-frequency sound scattered from an interrogation volume^{1,2}, and the other, computationally simulating molecular dynamic systems^{6,7}. The results from the present experiment are significant since they show that molecular hydrodynamic processes can now be directly observed using macroscopic experimental measurements of vibrated grain pile dynamics. Equally significant, macroscopic statistical mechanical and continuum flow models that were developed in this study allow consistent, quantitative interpretation and prediction of equilibrium and non-equilibrium, single-grain and multi-grain dynamics. Now, an experimentalist can study these processes directly, bypassing, for example, computationally expensive simulations, or technically challenging molecular-scale particle scattering measurements. Furthermore, the theoretical framework developed here can be used to justify computational fluid dynamic (CFD) modeling in similar flows¹⁴.

Future applications

The macroscopic experimental methods and theoretical models developed here can also be used to study various mass finishing processes, *e.g.*, vibratory finishing¹⁴, which are important in the manufacture of a large range of mechanical components. Additionally, the fundamental work begun here will continue as we explore dynamical connections between vibrated, high-restitution grain piles and liquid-state molecular hydrodynamic systems. A model utilizing the discrete element method (DEM) is also under development and will be used to model the three-dimensional dynamical behavior of vibratory finishing processes, as well as computationally studying the molecular hydrodynamics of vibrated grain systems. [DEM differs from computational fluid dynamics (CFD) in that CFD simulations are governed by the NS equations, while DEM models are governed by collisional Newtonian particle dynamics.]

Critical steps in the protocol

The most critical steps in this protocol from the beginning is the initial set up or the overall system, specifically the camera location with respect to the bowl, lighting should be diffuse so that it evenly covers the FOV, verify there are no reflections that cause glare in the images, steady FC flow and calibration of the PIV system. When setting up the bowl and the camera tripod/scaffolding, it must be verified that the vibratory system does not touch any portion of the camera or camera support system to ensure that the camera remains absolutely steady throughout the testing. Adequate lighting must be present on the entire test area to ensure the camera can pick up individual pieces of media throughout the test and that shadows do not create additional ghost pieces. An initial amount of solution must be dumped over the media prior to starting the vibratory system to ensure the media is "lubricated" and does not stick together at the beginning of the test. If the pieces stick together, they no longer represent molecules impacting each other, and they cause friction, which wears down the media and alters their size and mass. If the calibration

of the PIV system, or the variables are not entered into the system correctly, the system will give false vector direction and magnitudes. To ensure the calibration is accurate, the ruler must be perpendicular to the camera with the scale easily readable in the image.

Disclosures

The authors have nothing to disclose.

Acknowledgements

This work was supported by the Office of Naval Research (ONR N00014-15-1-0020)[Tkacik and Keanini] and performed at the University of North Carolina at Charlotte's Motorsports Research Lab. Polishing media was donated by Rosler.

References

1. Berne, B. J., & Pecora, R. *Dynamic Light Scattering*, John Wiley and Sons Ltd. (1976).
2. Boon, J. P., & Yip, S. *Molecular Hydrodynamics*. McGraw-Hill (1980).
3. Brown, J. C., Pusey, P. N., Goodwin, J. W., & Ottewill, R. H. Light scattering study of dynamic and time-averaged correlations in dispersions of charged particles. *J. Phys. A: Math Gen.* **Vol 5** (8) , 664-682 (1975).
4. Wainwright, T. E., Alder, B. J., & Gass, D. M. Decay of time correlations in two dimensions. *Phys. Rev.A.* **4**, 233-236 (1971).
5. Evans, D. J., & Morriss, G. P. *Statistical Mechanics of Nonequilibrium Liquids*., ANU E Press (2007).
6. Levesque, D., & Verlet, L. Computer "experiments" on classical fluids, III. time-dependent self correlation functions. *Phys. Rev. A.* **2**, 2514-2528 (1970).
7. Levesque, D., & Ashurst, W. T. Long-time behavior of the velocity autocorrelation function for a fluid of soft repulsive particles. *Phys. Rev. Lett.* **33**, 277-280 (1970).
8. Lovesey, S. W. *Dynamics of solids and liquids by neutron scattering*. Lovesey, S. W., & Springer, T. eds, Springer-Verlag (1977).
9. Forster, D. *Hydrodynamic fluctuations, broken symmetry, and correlation functions*. Perseus (1990).
10. Mountain, R.D. Generalized hydrodynamics. *Adv. Mol.Relax. Processes.* **9**, 225-291 (1977).
11. Zwanzig, R. Time-correlation functions and transport coefficients in statistical mechanics. *Ann. Rev. Phys. Chem.* **16**, 67-102 (1965).
12. Keanini, R. G. *et al.* Macroscopic liquid-state molecular hydrodynamics. *Sci. Rep.* **7**, 41658; (2017).
13. Kushick, J., & Berne, B.J. Role of attractive forces in self-diffusion in dense Lennard-Jones fluids. *J. Chem. Phys.* **59**(7), 3732-3736 (1973).
14. Mullany, B. *et al.* The application of computational fluid dynamics to vibratory finishing processes, *CIRP Annals.* (2017).
15. Fleischhauer, E., Azimi, F., Tkacik, P.T., Keanini, R.G & Mullany, B. Application of particle imaging velocimetry (PIV) to vibrational finishing. *J. Mater. Process. Technol.* **229**, 322-328 (2016).
16. Navare, J. *Experimental and computational evaluation of a vibratory finishing process*. MSME thesis, University of North Carolina at Charlotte, Charlotte, NC. (2017).
17. Bolmatov, V., Brazhkin, V., & Trachenko, K. The phonon theory of liquid thermodynamics. *Sci. Rep.* **2**, 421 (2012).
18. Elton, D. C., & Fernandez-Serra, M. The hydrogen-bond network of water supports propagating optical phonon-like modes. *Nat. Commun.* **7**, 10193 (2016).
19. Pathria, R. K., & Beale, P. D. *Statistical mechanics*. 3rd ed. Elsevier (2011).
20. Gibbs, J. W. *Elementary principles in statistical mechanics*. University Press (1902).
21. Toda, M., Kubo, R., & Saito, N. *Statistical physics I, 2nd ed.* Springer-Verlag (1992).
22. Kubo, R., Statistical mechanical theory of irreversible processes. *I. J. Phys. Soc. Japan.* **12**, 570-586 (1957).
23. Kubo, R., Toda, M., & Hashitsume, N. *Statistical physics II: nonequilibrium statistical mechanics*. Springer (1991).